Received: 15 February 2021 | Accepted: 4 March 2021

DOI: 10.1002/jsid.1006

SPECIAL SECTION PAPER

WILEY

Compact, fast-response, continuous, and wide-angle laser beam steerers

Ziqian He, SID Student Member | **Shin-Tson Wu, SID Fellow**

College of Optics and Photonics, University of Central Florida, Orlando, Florida, USA

Correspondence
Shin-Tson Wu, College of Optics and Photonics, University of Central Florida, Orlando, Florida, USA.
Email: swu@creol.ucf.edu

Funding information
Air Force Office of Scientific Research, Grant/Award Number: FA9550-14-1-0279

Abstract

A liquid crystal-cladding waveguide with resistive electrode configuration is proposed for laser beam steering applications. It can achieve wide-angle, continuous coverage, two-dimensional beam control with fast response time. With numerical validation, we find that in comparison with previous prismatic electrode approach, our device demonstrates higher compatibility with high birefringence liquid crystal materials, and thus, a more compact form factor can be realized. Such a beam steerer is attractive for a wide range of applications including automotive LiDAR, eye-tracking for near-eye displays, and high-precision 3D printing.

KEYWORDS

liquid crystal waveguides, nonmechanical beam steering, resistive electrodes

1 | INTRODUCTION

Nonmechanical laser beam steering,[1,2] as shown in Figure 1, is pivotal for light detection and ranging (LiDAR), eye-tracking in near-eye displays, high-precision 3D printing, microscopy, and optical tweezers.[3–8] In the past decade, several approaches have been developed, including liquid crystal (LC)-based optical phased arrays (OPAs), solid-state OPAs, LC-cladding waveguides, and so on.[9–14] However, it is still challenging to achieve high-precision, large aperture size, wide field of view (FOV), and high efficiency. Recent development of autonomous vehicles further promotes the demand for high-speed and high-precision nonmechanical beam steerers. Among all the choices, LC-cladding waveguides[15] and active LC-metasurfaces[16] are currently two promising options.

The refractive LC-cladding waveguide developed by Vescent Photonics[15] offers several attractive features: (1) 1D beam steerer with a remarkable steering range of 270°, (2) a wide-angle continuous coverage 2D beam steerer (50° × 15°), (3) high speed scanning (60 kHz), and (4) a large aperture scanner (1.2 cm demonstrated). The reason this device can achieve such a fast response time is because the evanescent field of the fundamental waveguide mode interacts with the LC layer near the surface of the waveguide core where the ultrathin LC layer is strongly anchored. As a result, the response time is in the order of 10 s μs. Moreover, the waveguide is 3–5 mm long, so the accumulated phase can exceed 1000 waves. In this paper, we propose and numerically validate an improved LC-cladding waveguide structure. With our high birefringence LC material, the proposed LC-cladding waveguide is promising for compact, high-precision, wide-angle, continuous, and high-speed beam steering.

2 | LC-CLADDING WAVEGUIDES

The system configuration of Vescent Photonics' LC-cladding waveguide is schematically plotted in Figure 2. It can achieve two-dimensional beam steering, with each dimension controlled by a separate module. Here, we mark them as in-plane steering (horizontal) and out-of-plane steering (vertical).

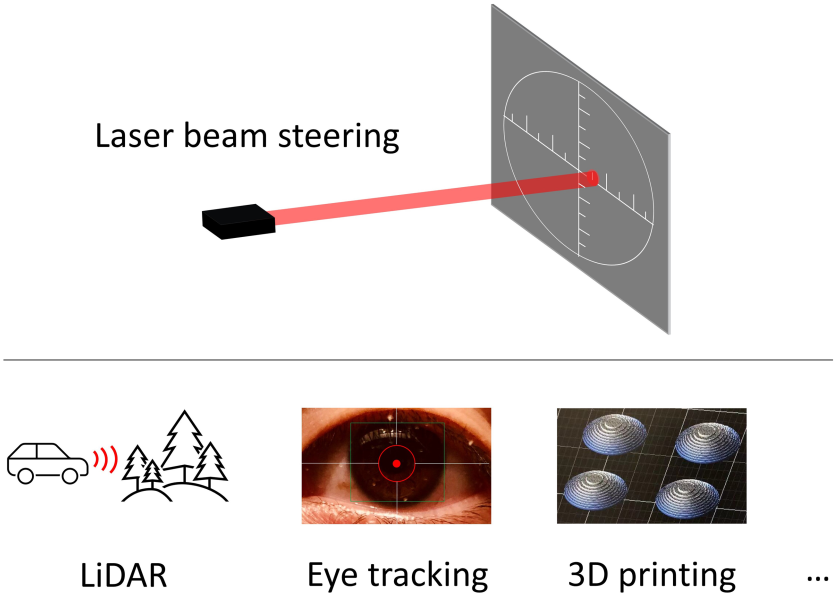

FIGURE 1 Nonmechanical laser beam steering technology for LiDAR, eye-tracking, 3D printing, and so forth

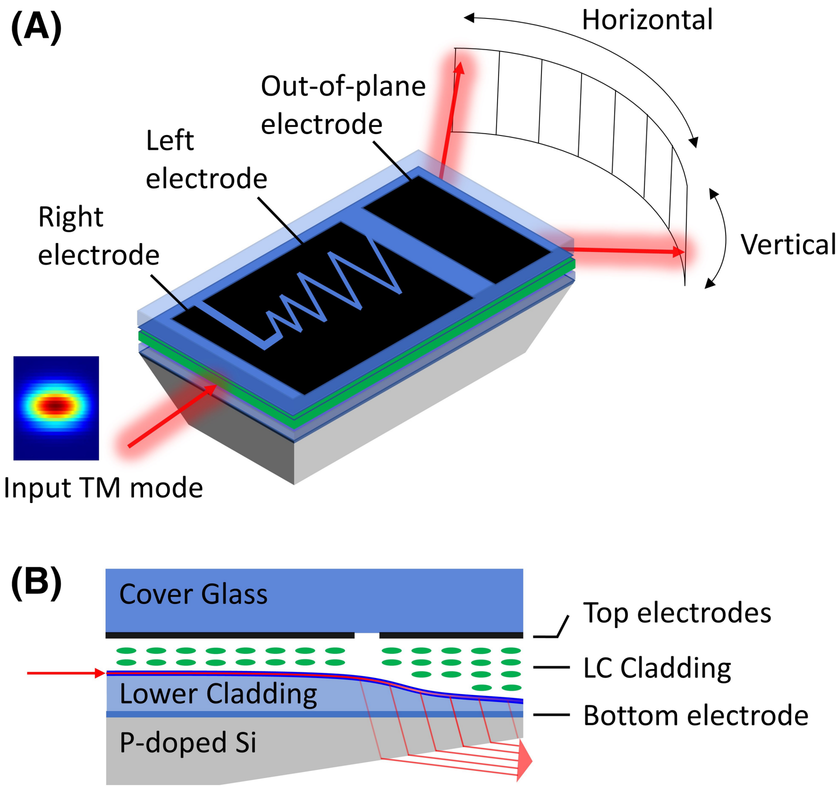

FIGURE 2 (A) Perspective view and (B) side view of the LC-cladding waveguide with prismatic electrodes. Inset in (A) shows the typical electric field intensity distribution of a fundamental TM mode

The first step for this beam steerer to work is to couple the laser beam into the waveguide. Note that the waveguiding mode is fundamental transverse magnetic (TM) in order to be compatible with the LC director modulation and to have single mode operation. From the side view (Figure 2B), the system, from top to bottom, consists of a cover glass, top electrodes and LC alignment, LC cladding, LC alignment and waveguide core, subcladding, bottom electrode, and a bottom substrate. In the LC cladding part, the LC directors are uniformly aligned along the light propagation direction. At the null voltage state, the LC cladding has a refractive index of n_o (ordinary refractive index). Whereas in the voltage-on state, the TM mode experiences a refractive index of n_e (extraordinary refractive index). In between, an effective refractive index applies. Because most energy is confined in the core, only a small portion of energy is extended to the LC cladding and get modulated. Consequently, the

LC cladding layer can be thin (~μm) and a fast response time can be obtained.

In such a system configuration, the laser beam is first steered in the in-plane direction by a pair of prismatic electrodes. Figure 3A depicts the top view of the electrodes. By applying a voltage to the left electrode, the beam direction is steered toward left. Similar mechanism holds for the right electrode. Figure 3B shows an example of refractive index distribution when only the left electrode is fully turned on. The light direction changes when passing through a prism with a refractive index contrast between the prism and the surrounding.

After the beam direction is tuned by the prismatic electrodes, the light will be gradually coupled out by a tapered sub-cladding and then leak into air. The vertical direction can be slightly modified by applying different voltages on the out-of-plane electrode. A 50° (horizontal) by 15° (vertical) steering range has been reported for $\lambda = 1.55$ μm.

3 | RESISTIVE ELECTRODE CONFIGURATION

In the original Vescent Photonics' design, prismatic electrodes are applied to provide the beam direction change. In this configuration, beam direction changes when refracting through each refractive index interface, and such change depends on the prism apex angle and refractive index contrast. When a larger beam steering angle is desired, the prism apex angle can be enlarged, but the size of each prism is also magnified. Consequently, it has limited freedom to shrink the form factor of the beam steerer.

Here, we demonstrate a modified device configuration, where instead of the prismatic electrodes, a resistive electrode is employed to steer the beam in plane. As shown in Figure 4, the resistive electrode is deposited between two conductive electrodes. When one of the conductive electrodes is applied with a high voltage and the other is applied with a low voltage (slightly lower than the threshold voltage), a gradient electric potential can be established across the resistive electrode. An example of refractive index distribution is plotted in Figure 4B, where the refractive index gradually decreases from bottom to top. This is achieved by applying a high voltage on the bottom conductive electrode. Previously, many have reported that an almost linear refractive index change can be established across the resistive electrode by carefully choosing the resistive materials.[17–19] In this case, light direction change is no longer caused by refracting through discrete refractive index contrast interfaces, but by continuous phase gradient accumulation. As we will discuss later, the advantage of using resistive electrode is its potential to reduce the form factor of the device.

4 | DEVICE SIMULATIONS

To prove concept and compare the performance of these two in-plane electrode designs, a series of numerical

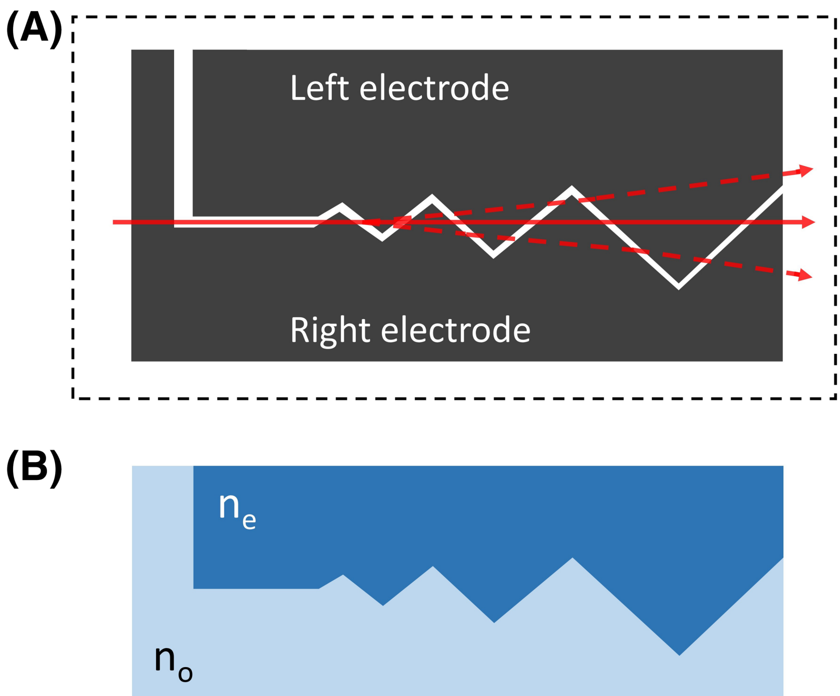

FIGURE 3 (A) Top view of the prismatic electrodes. (B) LC refractive index distribution (TM mode) when the left electrode is fully turned on

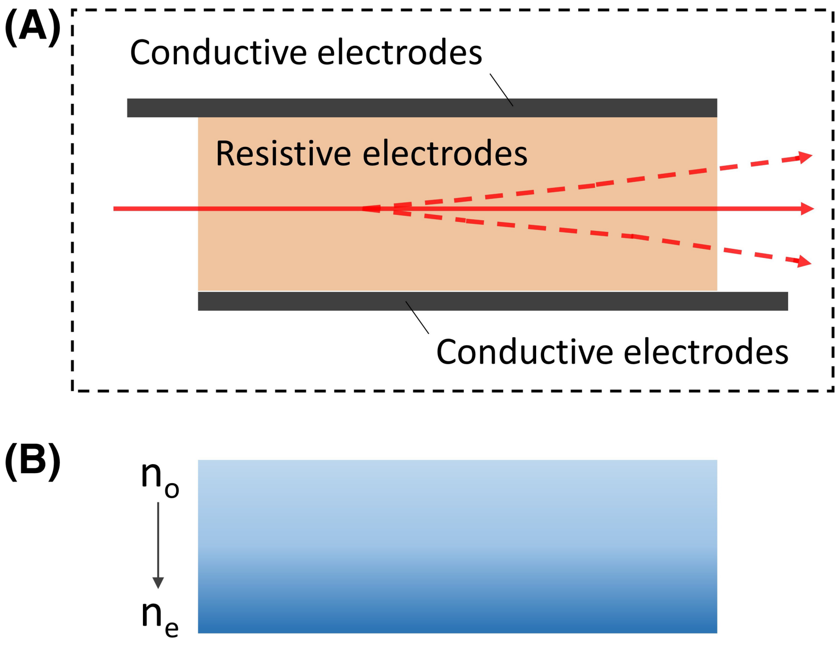

FIGURE 4 (A) Top view of the conductive electrodes. (B) An example of LC refractive index distribution (TM mode) when the bottom conductive electrode is turned on

simulations are conducted using the finite-difference time-domain method. The parameters used in our simulation are listed as follows: the operation wavelength is 905 nm; the refractive index of the sub-cladding and core is 1.6 and 2.0, respectively; a 20-nm alignment layer with a refractive index of 1.5 is placed in between the waveguide core and LC cladding; the maximum birefringence of LCs is 0.36; the ordinary refractive index of LCs is 1.50; the thickness of the core is 400 nm. The choice of core thickness considers single TM mode operation in the waveguide.

In the simulation of the resistive electrode configuration, the electrode width is assumed to be 60 μm and a linear polar angle transition from 0° (parallel to waveguide) to 90° (perpendicular to waveguide) is established under the resistive electrode. Note that a linear polar angle transition does not correspond to a linear refractive index transition in the cladding. The refractive index transition can be obtained using the polar angle information shown below[20]:

$$n_{eff} = \frac{n_o n_e}{\sqrt{n_e^2 \cos^2 \alpha + n_o^2 \sin^2 \alpha}}. \tag{2}$$

In Equation 2, n_o and n_e stand for the ordinary and extraordinary refractive indices of the LC, and α is the polar angle.

Meanwhile, we also estimate the performance of the prismatic electrode configuration and compare it with the resistive electrode design. In the simulation, all the prisms share the same shape and size: the prism apex angle is 5° and the distance between two neighboring prisms is 8 μm. To study the performance trend, a short propagation distance of 24 μm is applied to both configurations. The beam steering performance including steering angle and power loss is plotted in Figure 5, as a function of Δn.

As the LC birefringence increases, the steering angle of the prismatic electrode configuration increases almost linearly, while that of the resistive electrode design grows even more rapidly. Apparently, for both configurations, a higher Δn LC material is more favorable to increase the steering angle within a limited space. Interestingly, the resistive electrode design gains more from a higher Δn LC material. On the other hand, light efficiency is also an important indicator of the beam steering performance. Since we are targeting at near IR beam steerers, the intrinsic absorption loss from LC materials is negligible.[21] The light efficiency loss presented in the simulation is mainly associated with the leaky modes in the waveguide, caused by interface refraction or gradual light direction changes. From Figure 5B, the energy loss in the resistive electrode design stays at a low level, whereas that in the prismatic electrode design increases dramatically as the LC Δn increases. This means, the prismatic electrode design will be very energy-inefficient if a large Δn LC material is employed.

The above simulation results are based on a propagating distance of 24 μm. In real cases, the propagating distance is much longer, reaching the order of ~mm or ~cm. We confirmed by the simulation that if the propagating distance increases, the steering angle enlarges linearly if the steering angle remains smaller than 5°.

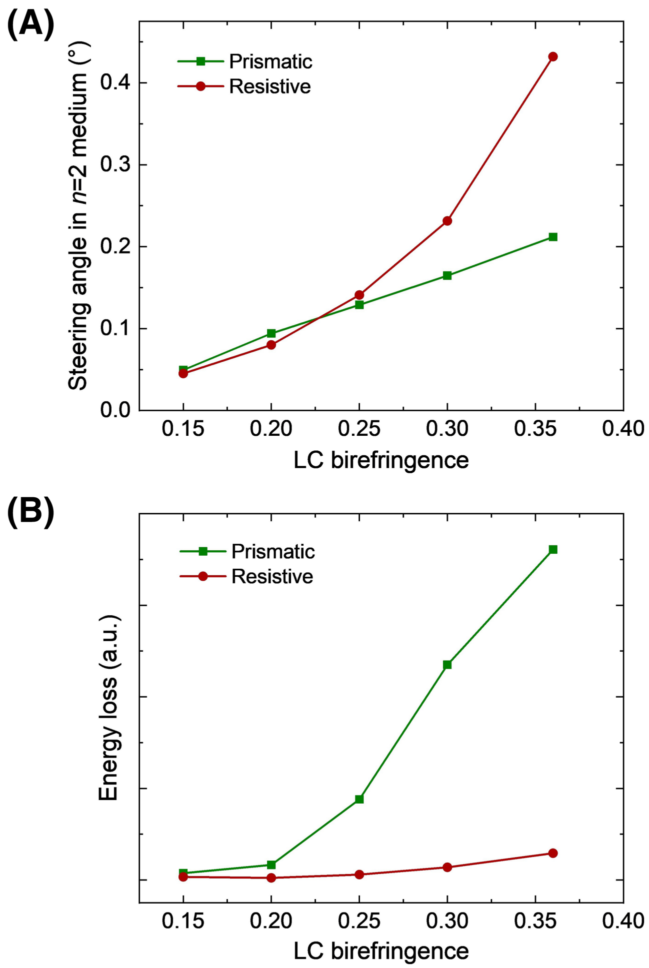

FIGURE 5 (A) Simulated steering angles in a medium with a refractive index of 2, as a function of LC Δn. (B) Simulated relative energy loss of LC-cladding waveguides as a function of LC Δn. Note that here the propagating distance is only 24 μm. In real cases, a ~mm scale can be used

To further enlarge the steering angle, a modified resistive electrode configuration can be employed, as will be discussed in next section. As a reference, a theoretical prediction on the relationship between steering angle and the arc length of resistive electrode is shown in Figure 6. The horizontal dimension of the waveguide structure is also depicted in Figure 6. Because we are using a curved resistive electrode here, the horizontal dimension will become smaller than the arc length of the resistive electrode, especially for larger steering angles. Meanwhile, as the propagating distance increases, the energy loss grows exponentially, following Beer's law. Considering both the steering angle range and optical efficiency, the resistive electrode design with high Δn LC materials will be a good choice. Fortunately, our group has developed several high Δn LC materials. For LiDAR at λ = 905 nm, an LC Δn as large as ~0.355 can be expected,[22] as Figure 7 shows.

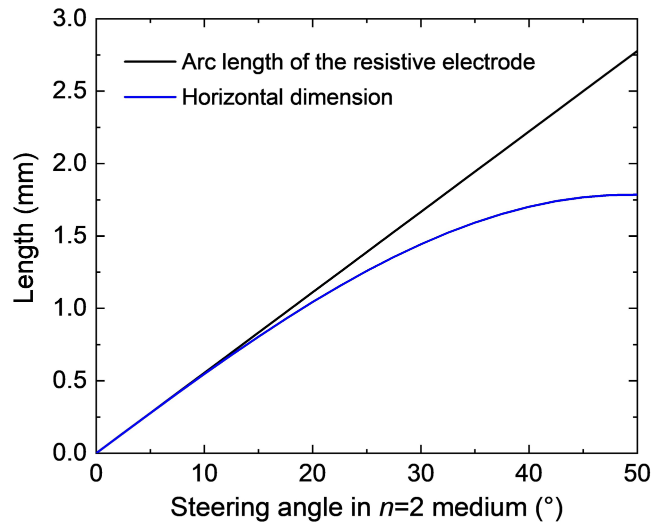

FIGURE 6 A theoretical prediction of the arc length of the resistive electrode and horizontal dimension of the waveguide as a function of steering angle in a high refractive index medium ($n = 2$)

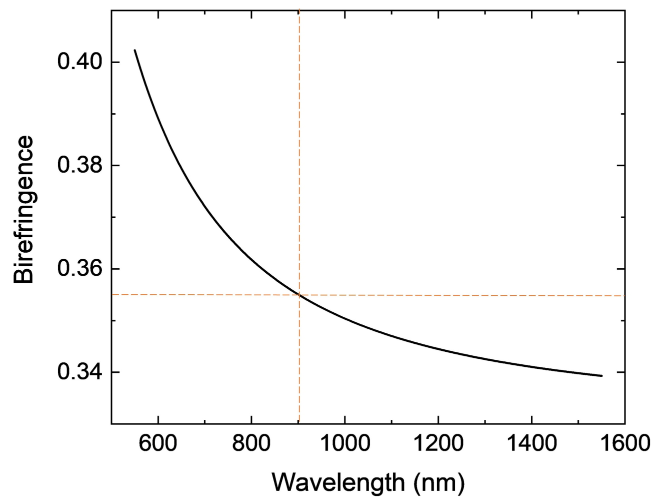

FIGURE 7 Birefringence dispersion of a high Δn LC mixture developed by our group

5 | DISCUSSION

Although the idea of the resistive electrode configuration is numerically validated, some challenges still need to be overcome. For example, in the simulation, we assume that the resistive electrode is straight. This may be fine for a small steering angle. If a larger steering angle is needed, a straight resistive electrode may cause problems. Since the guided beam will shift left/right while propagating in the waveguide, after some propagation distance, the beam could shift out of the resistive electrode area. A possible solution is to design a left/right track using

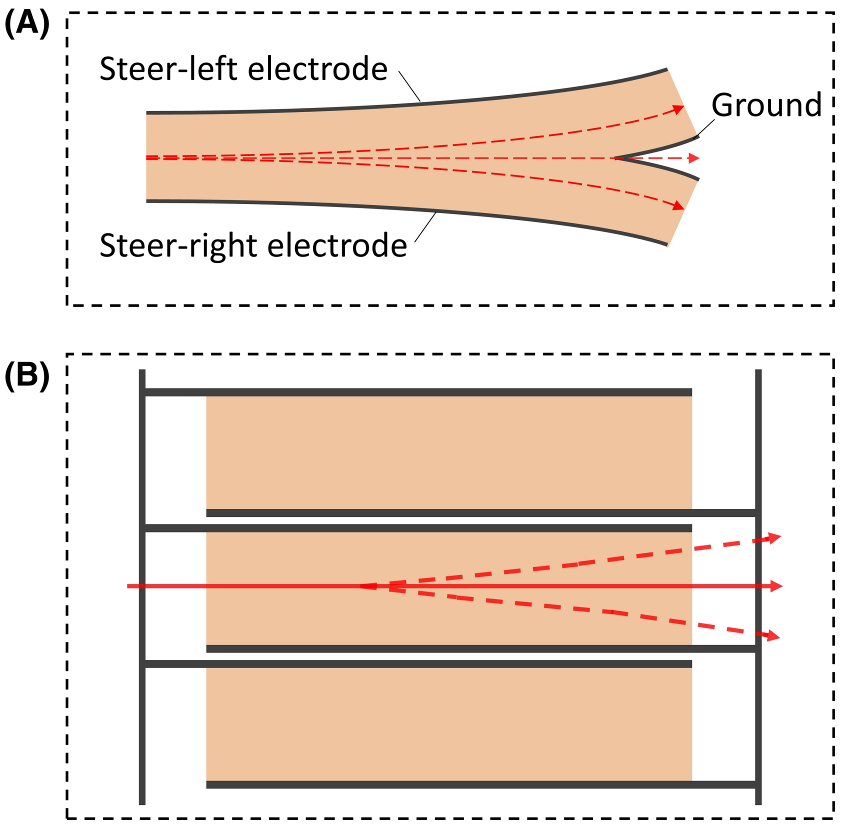

FIGURE 8 (A) Schematic of the curved resistive electrode design for a larger steering range. (B) Schematic of the refractive Fresnel resistive electrode design for a larger aperture size

patterned resistive electrodes, as Figure 8A shows. In this modified configuration, three electrodes are utilized. To steer the beam to the left, a high voltage is applied to steer-left electrode, and a low voltage (~threshold voltage of LCs) is applied to steer-right and ground electrodes. When the steer-left electrode is at on-state, the laser beam will follow the designed track. While it is at intermediate states (e.g., applied voltage < on-state voltage), the beam will leak out the track by passing through the ground electrode at some position. Ideally, by controlling the steer-left electrode, the steering angle can be continuously tuned. This working principle can be similarly utilized to steer the beam to the right.

Another concern is the limited aperture. In our simulation, an electrode width of 60 μm was assumed. If the input beam size is large than 60 μm, only part of the energy in the resistive electrode area will be modulated. Even though simply increasing the resistive electrode width may alleviate such limitation, the steering angle will be decreased due to the reduced refractive index gradient. A possible configuration to increase the aperture is shown in Figure 8B. Instead of only one resistive electrode, a group of resistive electrodes can be designed. The working mechanism is similar to a refractive Fresnel lens, where after each block of resistive electrodes, the phase of light undergoes a reset. The downside is the existence of flyback areas between two blocks, which will inevitably cause energy loss and some beam profile distortion. Yet this trade-off needs to be further evaluated.

6 | CONCLUSION

We proposed a resistive electrode-based LC cladding waveguide for non-mechanical beam steering. Finite-difference time-domain simulation models were established to evaluate its performance. Compared to the previous prismatic electrode design, our device shows higher compatibility with high birefringence LC materials and thus can potentially achieve a more compact beam steerer with a lower energy loss. We also proposed some electrode designs to further enlarge the steering range and acceptance aperture size. The resistive electrode-based LC cladding waveguides can potentially offer compact, fast-response, continuous, and wide-angle laser beam steering features that are ideal for practical applications such as LiDAR, near-eye displays, and beyond.

FUNDING INFORMATION

The authors are indebted to Air Force Office of Scientific Research (AFOSR) for the financial support under grant FA9550-14-1-0279.

ORCID

Ziqian He https://orcid.org/0000-0003-3560-2987
Shin-Tson Wu https://orcid.org/0000-0002-0943-0440

REFERENCES

1. McManamon PF, Bos PJ, Escuti MJ, et al. A review of phased array steering for narrow-band electrooptical systems. Proc IEEE. 2009;97(6):1078–1096.
2. He Z, Gou F, Chen R, Yin K, Zhan T, Wu ST. Liquid crystal beam steering devices: principles, recent advances, and future developments. Crystals. 2019;9(6):292.
3. Hair JW, Hostetler CA, Cook AL, et al. Airborne high spectral resolution lidar for profiling aerosol optical properties. Appl Optics. 2008;47(36):6734–6752.
4. Duchowski AT, Shivashankaraiah V, Rawls T, Gramopadhye AK, Melloy BJ, Kanki B. Binocular eye tracking in virtual reality for inspection training. Proc ETRA. 2000; 89–96.
5. He Z, Tan G, Chanda D. Wu ST. Novel liquid crystal photonic devices enabled by two-photon polymerization. Opt Express. 2019;27(8):11472–11491.
6. Betzig E, Trautman JK. Near-field optics: Microscopy, spectroscopy, and surface modification beyond the diffraction limit. Science. 1992;257(5067):189–195.
7. Neuman KC, Block SM. Optical trapping. Rev Sci Instrum. 2004;75(9):2787–2809.
8. Gattass RR, Mazur E. Femtosecond laser micromachining in transparent materials. Nat Photonics. 2008;2(4):219–225.
9. Resler DP, Hobbs DS, Sharp RC, Friedman LJ, Dorschner TA. High-efficiency liquid-crystal optical phased-array beam steering. Opt Lett. 1996;21(9):689–691.
10. Poulton CV, Yaacobi A, Cole DB, et al. Coherent solid-state LIDAR with silicon photonic optical phased arrays. Opt Lett. 2017;42(20):4091–4094.
11. Frantz JA, Myers JD, Bekele RY, et al. Chip-based non-mechanical beam steerer in the midwave infrared. J Opt Soc am B. 2018;35(12):C29–37.
12. Kim J, Oh C, Serati S, Escuti MJ. Wide-angle, nonmechanical beam steering with high throughput utilizing polarization gratings. Appl Optics. 2011;50(17):2636–2639.
13. Yin K, Zhan T, Xiong J, He Z, Wu ST. Polarization volume gratings for near-eye displays and novel photonic devices. Crystals. 2020;10(7):561.
14. Yousefzadeh C, Van Rynbach A, Bryant D, Bos P. High-efficiency, tunable, fringe-field switching-mode beam steering based on a liquid crystal Pancharatnam phase. Appl Optics. 2020;59(34):10706–10718.
15. Davis SR, Farca G, Rommel SD, Johnson S, Anderson MH. Liquid crystal waveguides: new devices enabled by >1000 waves of optical phase control. Proc SPIE. 2010;7618:76180E.
16. Li SQ, Xu X, Veetil RM, Valuckas V, Paniagua-Domínguez R, Kuznetsov AI. Phase-only transmissive spatial light modulator based on tunable dielectric metasurfaces. Science. 2019;364 (6445):1087–1090.
17. Li Y, Liu Y, Li Q, Wu ST. Polarization independent blue-phase liquid crystal cylindrical lens with a resistive film. Appl Optics. 2012;51(14):2568–2572.
18. Shang X, Trinidad AM, Joshi P, De Smet J, Cuypers D, De Smet H. Tunable optical beam deflection via liquid crystal gradient refractive index generated by highly resistive polymer film. IEEE Photonics J. 2016;8(3);1–11.
19. Beeckman J, Nys I, Willekens O, Neyts K. Optimization of liquid crystal devices based on weakly conductive layers for lensing and beam steering. J Appl Phys. 2017;121(2): 023106.
20. He Z, Yin K, Xiang EL, Wu ST. Birefringent light-shaping films for mini-LED backlights. J Soc Inf Disp. 2020;28(6):476–482.
21. Wu ST. Absorption measurements of liquid crystals in the UV, visible and infrared. J Appl Phys. 1998;84(8):4462–4465.
22. Gauza S, Li J, Wu ST, et al. High birefringence and high resistivity isothiocyanate-based nematic liquid crystal mixtures. Liq Cryst. 2005;32(8):1077–1085.

AUTHOR BIOGRAPHIES

Ziqian He received his BS degree in Materials Physics from Nanjing University in 2016 and is currently working toward a PhD degree from the College of Optics and Photonics, University of Central Florida. His current research interests include novel liquid crystal devices, nanocrystals, and color science.

Shin-Tson Wu is Pegasus Professor at the College of Optics and Photonics, University of Central Florida. He is among the first six inductees of the Florida Inventors Hall of Fame (2014) and a Charter Fellow of the National Academy of Inventors (2012). He is a Fellow of the IEEE, OSA, SID, and SPIE, and an honorary Professor of Nanjing University (2013) and of National Chiao Tung University (2018). He is the recipient of 2014 OSA Esther Hoffman Beller Medal, 2011 SID Slottow-Owaki Prize, 2010 OSA Joseph Fraunhofer Award, 2008 SPIE G. G. Stokes Award, and 2008 SID Jan Rajchman Prize.

How to cite this article: He Z, Wu S-T. Compact, fast-response, continuous, and wide-angle laser beam steerers. *J Soc Inf Display*. 2021;29:281–287. https://doi.org/10.1002/jsid.1006